

## A NEW PROBE OF THE PLANET-FORMING REGION IN T TAURI DISKS

EDWIN BERGIN,<sup>1</sup> NURIA CALVET,<sup>2</sup> MICHAEL L. SITKO,<sup>3,4</sup> HERVE ABGRALL,<sup>5</sup> PAOLA D’ALESSIO,<sup>6</sup> GREGORY J. HERCZEG,<sup>7</sup>  
EVELYNE ROUEFF,<sup>5</sup> CHUNHUA QI,<sup>2</sup> DAVID K. LYNCH,<sup>4,8</sup> RAY W. RUSSELL,<sup>4,8</sup> SUELLEN M. BRAFFORD,<sup>4,9</sup> AND R. BRAD PERRY<sup>4,10</sup>

Received June 23; accepted September 10; published 2004 September 20

### ABSTRACT

We present new observations of the far-ultraviolet (FUV; 1100–2200 Å) radiation field and the near- to mid-IR (3–13.5 μm) spectral energy distribution (SED) of a sample of T Tauri stars selected on the basis of bright molecular disks (GM Aur, DM Tau, and LkCa 15). In each source we find evidence for Ly $\alpha$ -induced H<sub>2</sub> fluorescence and an additional source of FUV continuum emission below 1700 Å. Comparison of the FUV spectra to a model of H<sub>2</sub> excitation suggests that the strong continuum emission is due to electron impact excitation of H<sub>2</sub>. The ultimate source of this excitation is likely X-ray irradiation that creates hot photoelectrons mixed in the molecular layer. Analysis of the SED of each object finds the presence of inner disk gaps with sizes of a few AU in each of these young (~1 Myr) stellar systems. We propose that the presence of strong H<sub>2</sub> continuum emission and inner disk clearing are related by the increased penetration power of high-energy photons in gas-rich regions with low grain opacity.

*Subject headings:* accretion, accretion disks — astrobiology — astrochemistry — circumstellar matter — stars: pre-main-sequence — ultraviolet: stars

*Online material:* color figure

### 1. INTRODUCTION

In recent years there has been growing evidence for evolution of solid particles in young ( $\leq 10$  Myr) protoplanetary accretion disks (Beckwith et al. 2000; D’Alessio 2003 and references therein). The onset of this evolution lies in the coagulation of submicron-sized particles into larger grains, a process that continues until the larger grains decouple from the gas and settle to a dusty midplane. In the midplane these solid particles grow in size until they become large enough to gravitationally focus collisions with smaller bodies, eventually making planets (Safonov 1972; Weidenschilling 1997).

Since dust grains within the disk absorb stellar UV and optical photons and reemit at wavelengths longer than  $\geq 2$  μm, the dust evolutionary process has direct consequences on disk continuum emission. Thus, at early evolutionary stages the presence of dust in the inner disk ( $\leq 10$  AU) is revealed by optically thick emission at near- and mid-IR wavelengths.

As grains grow the opacity at these wavelengths decreases, revealing stellar photospheric emission. The formation of giant planets can also affect the dust emission. Gravitational interaction between the disk and the forming planet results in the formation of a gap as the mass of the planet increases (Bryden

et al. 1999; Alibert et al. 2004 and references therein), producing a significant decrease in disk flux in the near-IR (Rice et al. 2003, hereafter R03).

What is less recognized, at least in terms of an observational signature, is that the molecular evolution is closely linked with the dust evolution. Disks in a more advanced degree of dust evolution will be more easily permeated by the destructive short-wavelength radiation fields generated in part by accretion. Since grain evolution and planet formation proceed more rapidly in the denser inner disk (Weidenschilling 1997), these effects will be magnified in the very regions that are closest to the source(s) of radiation. In this Letter we suggest that a strong H<sub>2</sub> UV emission feature is an observational consequence of grain growth/planet formation in the inner disks of young ( $\sim 10^6$  yr) accreting T Tauri disks.

### 2. OBSERVATIONS

The sources chosen for the Space Telescope Imaging Spectrograph (STIS) UV study are DM Tau, GM Aur, and LkCa 15. In Table 1 we provide some basic characteristics for these systems. All sources have relatively similar properties and were selected on the basis of the presence of gas disks with rich molecular complexity (Koerner et al. 1993; Dutrey et al. 1997; Qi et al. 2003). Each are single star systems with no evidence for binary companions (White & Ghez 2001). *Hubble Space Telescope (HST)* STIS spectra of DM Tau, LkCa 15, and GM Aur were obtained for *HST* program G09374 on 2003 February 5, February 13, and April 1, respectively. Exposures were taken using the G140L (1150–1730 Å) and G230L (1570–3180 Å) gratings with an aperture size of 2". The spectral resolution per pixel for G140L is  $\Delta\lambda = 0.6$  and 1.58 Å for G230L. With a FWHM of the point-spread function of 1.5 pixels at the far-ultraviolet (FUV) and 2 pixels at the near-ultraviolet (NUV), this results in effective resolutions of 0.9 Å ( $R \sim 1550$ ) at the FUV and 3 Å in the NUV ( $R \sim 770$ ). The plate scale is 0".024 pixel<sup>-1</sup> in both FUV and NUV, so the aperture size is large enough for spectrophotometry. Exposure times were 10 m (G230L) and ~65 m (G140L) for DM Tau and GM Aur and 189 m

<sup>1</sup> Department of Astronomy, University of Michigan, 825 Dennison Building, 501 East University Avenue, Ann Arbor, MI 48109-1090; ebergin@umich.edu.

<sup>2</sup> Harvard-Smithsonian Center for Astrophysics, 60 Garden Street, Cambridge, MA 02138.

<sup>3</sup> Department of Physics, University of Cincinnati, 400 Geology/Physics Building, P.O. Box 210011, Cincinnati, OH 45221-0011.

<sup>4</sup> Visiting Astronomer, NASA Infrared Telescope Facility, operated by the University of Hawaii under contract with the National Aeronautics and Space Administration.

<sup>5</sup> Laboratoire Univers et Théories, UMR 8102 du CNRS, Observatoire de Paris, Section de Meudon, Place Jules Janssen, 92195 Meudon, France.

<sup>6</sup> Instituto de Astronomía, UNAM, Apartado Postal 72-3 (Xangari), 58089 Morelia, Michoacan, Mexico.

<sup>7</sup> JILA, University of Colorado, 440 UCB, Boulder, CO 80309-0440.

<sup>8</sup> The Aerospace Corporation, P.O. Box 92957, Los Angeles, CA 90009-2957.

<sup>9</sup> School of Law, University of Dayton, 300 College Park, Dayton, OH 45469-2760.

<sup>10</sup> NASA Langley Research Center, Mail Stop 111, Hampton, VA 23681-2199.

TABLE 1

STELLAR PROPERTIES AND MODEL RESULTS			
Parameter	GM Aur	LkCa 15	DM Tau
Stellar Properties			
SpT .....	K3	K5	M1
$T_{\text{eff}}$ .....	4730	4350	3720
$A_V$ .....	0.14	0.62	0.9
$L$ .....	0.83	0.74	0.25
$R_*$ .....	1.35	1.51	1.20
$\log L_{\text{acc}}$ .....	-1.149	-1.055	-1.749
$\log \dot{M}$ .....	-8.563	-8.096	-9.103
$G_0$ .....	340	1500	240
Model Results			
$R_i/\text{AU}$ .....	6.5	3	4
$T_w/K$ .....	124	177	117
$z_w/R$ .....	0.12	0.03	0.13
$\tau_{\text{min}}$ .....	0.005	0.007	0.007
$R_d/R_*$ .....	12	9.8	12
$z_{\text{dust}}/R_d$ .....	0.01	0.08	0.006

NOTES.— $G_0$  = field at 100 AU in Habing; 1 Habing = standard UV flux from interstellar radiation field. Stellar data in solar units are from KH95.

(G140L) and 37 m (G230L) for LkCa 15. Standard CALSTIS pipeline procedures were used to reduce the data.<sup>11</sup>

The targets were observed in the mid-IR over the course of three separate observing runs (2003 January and February) that overlapped the *HST* observations for DM Tau and LkCa 15 (5–6 week difference for GM Aur). Observations were obtained with the Aerospace Corporation's Broadband Array Spectrograph System (BASS; Sitko et al. 2000) with a 3/4 beam on the NASA Infrared Telescope Facility.

This instrument uses a cold beam splitter to separate the light into two separate wavelength regimes (2.9–6 and 6–13.5  $\mu\text{m}$ ). Each beam is dispersed onto a 58 element blocked impurity band linear array, thus allowing for simultaneous coverage from 2.9 to 13.5  $\mu\text{m}$ . The spectral resolution is wavelength dependent, ranging from  $R \sim 30$  to 125 over each wavelength region. Integration times were 40 minutes (GM Aur), 227 minutes (DM Tau), and 143 minutes (LkCa 15). All observations are calibrated relative to  $\alpha$  Tau, with typical air masses  $\sim 1.07$  and calibrator air masses ranging from 1.03 to 1.12.

### 3. RESULTS

#### 3.1. UV Spectra of T Tauri Stars

Figure 1 shows the FUV dereddened fluxes of the T Tauri stars in our sample including the spectra of TW Hya from Herczeg et al. (2002). In Table 1 we provide the strength of the FUV radiation at 100 AU (estimated by integrating the FUV radiation field from 1100 to 1700  $\text{\AA}$ ) normalized to that of the interstellar UV radiation field. This estimate is a lower limit because of the unknown Ly $\alpha$  flux.<sup>12</sup>

Figure 2 shows the spectrum of LkCa 15 with prominent emission features identified. In TW Hya (Fig. 1) there is a strong Ly $\alpha$  emission line that is not as evident in the other

<sup>11</sup> There is some overlap in wavelength coverage between the NUV and FUV detectors. No correction was needed to be applied to match flux levels, and the data are presented with overlap included. Some data were not shown at the short-wavelength end of the NUV spectra to better illustrate particular features. However, the NUV data in this spectral region closely mirror the FUV data.

<sup>12</sup> There is little information on the strength of the radiation field below 1100  $\text{\AA}$ . *Far Ultraviolet Spectroscopic Explorer* data of TW Hya indicate that the FUV field strength,  $G_0 = 3400$  (including Ly $\alpha$ ), does not change appreciably with this radiation included (Herczeg et al. 2004).

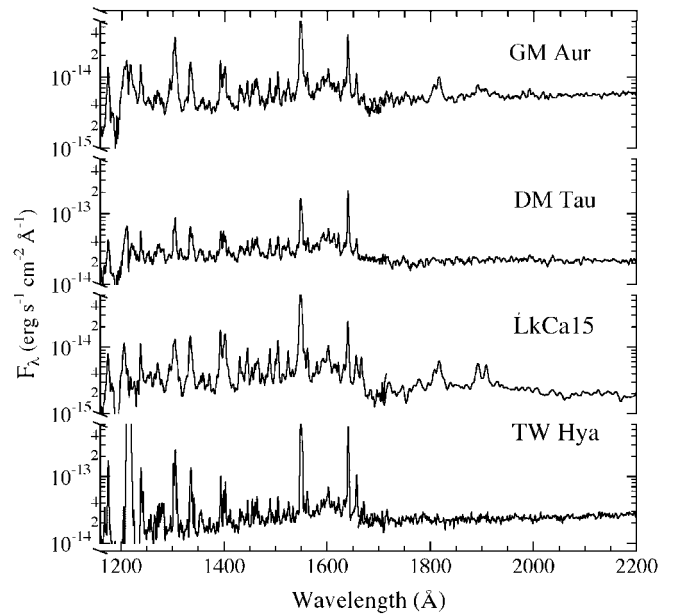


FIG. 1.—*HST* STIS spectra of objects in our sample, including the spectra of TW Hya first discussed in Herczeg et al. (2002) but with reduced spectral resolution (1.5  $\text{\AA}$ ).

sources because these sources are embedded within molecular clouds; in contrast TW Hya has no local cloud and little interstellar absorption (Herczeg et al. 2004). Evidence for strong Ly $\alpha$  radiation that penetrates to the molecular layer can be inferred from the presence of numerous emission features coincident with Ly $\alpha$  pumped H $_2$  emission lines. In Figure 2 some of these coincidences are denoted for LkCa 15, but similar features are seen in all sources shown in our sample. Beyond the clear H $_2$  emission-line features there also appears a sharp rise in emission below 1700  $\text{\AA}$ . This feature is likely due to a combination of *discrete and continuum* emission emitted by H $_2$  molecules in excited electronic states.

H $_2$  emission below 1700  $\text{\AA}$  can result from at least two physical mechanisms (e.g., Herczeg et al. 2004), Ly $\alpha$ -induced fluores-

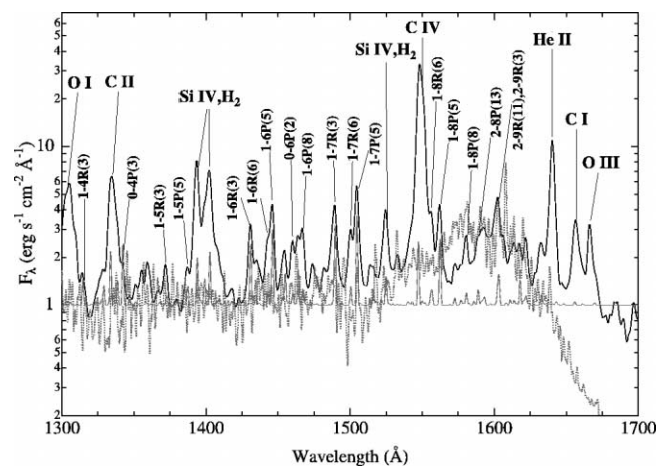


FIG. 2.—Comparison of observed LkCa 15 spectrum (*solid black line*), with strong features identified, the electron impact model spectrum (*dotted line*), and model of Ly $\alpha$  fluorescence (*solid gray line*). The model spectra were produced using an excitation model and molecular transition probabilities in the discrete and continuum range (Abgrall et al. 1994, 2000). For ease in comparison, the fluxes from both observation and models are normalized to the flux at 1425  $\text{\AA}$ . [See the electronic edition of the Journal for a color version of this figure.]

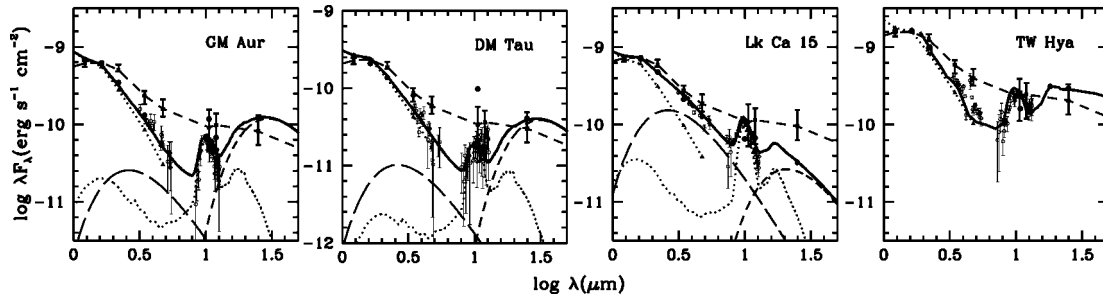


FIG. 3.—SEDs of GM Aur, DM Tau, and LkCa 15: BASS data (*small open circles*), optical, and *IRAS* bands from KH95 (*large filled circles*). Also shown are the photospheric fluxes (*filled triangles joined by dotted line*) and the contribution of the wall (*short-dashed lines*), the optically thin inner region (*dotted line*), and the possible rim at the dust destruction radius (*long-dashed line*). We show for comparison the median of Taurus (*filled rectangles joined by dashed lines*; error bars denote the quartiles of the distribution) from D’Alessio et al. (1999). The last panel shows the SED of TW Hya, with data and model from Calvet et al. (2002). Photospheric fluxes are calculated from standard colors and spectral types from KH95, scaled to the dereddened *J* magnitude of each object. Models discussed in § 3.2 are shown as solid lines. We do not include the contribution of the outer disk, which becomes important at longer wavelengths than those considered here (C02).

cence and electron impact excitation followed by fluorescence (Liu et al. 2002). Ly $\alpha$  excitation involves only the ungerade electronic states ( $B^1\Sigma_u$  and  $C^1\Pi_u$ ), producing a spectrum permeated by discrete emission lines with some continuum emission. However, electron impact excitation can also excite the gerade states ( $E$ ,  $F$ , etc.) that cascade toward the  $B$  and  $C$  states and emit subsequent UV fluorescence. This produces a broader spectrum with greater contribution from the  $H_2$  dissociation continuum (Abgrall et al. 1997; Jonin et al. 2000; Liu et al. 2003).

A model spectrum for the 100 eV electron impact spectrum is displayed in Figure 2. A simple comparison of our data to the electron impact model in Figure 2 shows similarities that are suggestive that electron impact excitation may be important.<sup>13</sup> The implications of this result are discussed in § 4.

### 3.2. Spectral Energy Distributions

The targets, selected on the basis of strong disk molecular emission, show indications of significant dust evolution in their inner disks. For example, the  $K - L$  colors of LkCa 15 and GM Aur are bluer than 86% of the Taurus sample (consisting of 51 classical T Tauri stars with near- and mid-IR observations from Kenyon & Hartmann 1995, hereafter KH95), and the  $K - L$  color of DM Tau is bluer than 70% of the sample. The BASS observations of the targets strengthen these indications. In Figure 3, we compare the mid-IR, optical, and *IRAS* data of the targets to the median spectral energy distribution (SED) of classical T Tauri stars in Taurus from D’Alessio et al. (1999). The SEDs of the targets show a clear flux deficit in the near-IR relative to the median in Taurus, analogous to that of TW Hya (cf. Fig. 3), for which inner disk clearing due to the action of a planet opening a gap in the disk has been suggested (§ 1; C02; R03).

Attempting to get insight into the structure of the inner region, we use a simple model, following C02 and Uchida et al. (2004). The model consists of (1) a vertical “wall” in the inner edge of the outer disk, representing the far edge of the gap. This wall, located at radius  $R_i$  with height  $z_w$ , is frontally illuminated by the star and emits as a blackbody with temperature  $T_w$ , where  $T_w = T_{\text{eff}}/R_i^{1/2}/2^{1/4}$  (cf. C02). We are ignoring the effects of geometry of the gap, inclination, and occultation.<sup>14</sup>

<sup>13</sup> In the electron impact model there is an additional strong feature near 1200 Å that we do not discuss because of the close proximity of Ly $\alpha$ . In a future publication we will compare the FUV spectra with  $H_2$  excitation models in greater detail.

<sup>14</sup> Emission from the wall in the disk is inclination dependent. However, the targets have inclinations  $\sim 30^\circ$ – $60^\circ$  (Simon et al. 2000; Qi et al. 2003), for which the wall emission is within 50% of the maximum (Dullemond et al. 2001).

(2) An optically thin inner disk, extending from the dust destruction radius to  $R_i$ , with optical depth  $\tau_{\text{min}}$  at 10  $\mu\text{m}$ . This region has a mixture of small ( $\sim 0.1 \mu\text{m}$ ) and large ( $\sim 2 \mu\text{m}$ ) grains, and we have added organics and troilite to the mostly amorphous silicate grains of Uchida et al. (2004). The optically thin dust temperatures are calculated from radiative equilibrium at each radius. The results of this simple modeling procedure are shown in Figure 3, where we show the spectrum of each individual component; model parameters are given in Table 1. It is clear in the case of LkCa 15 that the two components alone cannot account for the excess emission above photospheric fluxes in the near-IR; some excess can be seen in the case of GM Aur and DM Tau as well. We find that this excess can be explained by blackbody emission at  $T_d = 1400$  K, the dust destruction temperature (see Fig. 3). We suggest that the innermost region of the inner disk is optically thick and has a rim at the dust destruction radius from where this emission arises, as is the case in other young disks (Dullemond et al. 2001; Muzerolle et al. 2003, hereafter M03).

Several points can be extracted from our analysis: (1) All disks have cleared their inner regions up to few AU.<sup>15</sup> (2) The height of the wall  $z_w$  at  $R_i$  puts an upper limit to the height of the outer disk at that radius because the wall could be “puffed up” with the enhanced radiative heating. Compared with predictions from disk structure calculations, the low values of  $z_w/R_i$  in GM Aur and DM Tau are consistent with models with very significant grain growth (cf. Fig. 5 in D’Alessio et al. 2001). The much lower value of LkCa 15 cannot be explained by models with well-mixed gas and dust; it probably requires a significant amount of dust settling. (3) The column density of dust required to produce the silicate feature is  $\Sigma_d \sim \tau_{\text{min}}/\kappa(10 \mu\text{m}) \sim 0.001 \text{ g cm}^{-2}$ , with  $\kappa(10 \mu\text{m}) \sim 1 \text{ cm}^2 \text{ g}^{-1}$ . Using standard expressions for accretion disks (cf. M03), we can estimate the column density of gas in the inner disk from the mass accretion rate  $\dot{M}$ . With  $\dot{M} \sim 3 \times 10^{-9} M_\odot \text{ yr}^{-1}$  as representative of our objects (Table 1), we obtain  $\Sigma_{\text{gas}} \sim 20 \text{ g cm}^{-2}$  at 1 AU, for  $\alpha = 0.01$ ,  $T = 100$  K, and  $\dot{M} = 1 M_\odot$ , with a corresponding dust column of  $\sim 0.2 \text{ g cm}^{-2}$  (using the standard dust-to-gas mass ratio), much higher than detected. As discussed in C02, one possibility is that the remaining dust is locked up in larger bodies with low near-IR opacities.

<sup>15</sup> The location of the outer edge of the gap  $R_i$  for GM Aur is larger than that inferred by R03. These authors had only broadband colors and included the silicate emission as emission from the wall. With our better observations, the optically thin emission can be separated from the wall optically thick emission, which is much lower in the  $\sim 10 \mu\text{m}$  region.

(4) We can estimate the height  $z_{\text{dust}}$  of the rim at the dust destruction radius from the solid angle required to fit the emission, assuming a cylindrical geometry. The radius of this cylinder would be the dust destruction radius, which can be calculated from the stellar and accretion luminosities (M03; Table 1). We find  $z_{\text{dust}} \leq 0.1H$  (Table 1), with  $H \sim 0.1R$ , which is much lower than the height of the rim previously found in thick inner disks (Dullemond et al. 2001; M03). We note that blackbody emission alone can explain the near-IR excess (Fig. 3). This suggests that the innermost optically thick region has a small radial extent and moreover, may be in the shadow of the rim (Dullemond et al. 2001). Taken together, all these results suggest that the solids in the inner disks of the targets have experienced significant evolution.

#### 4. DISCUSSION

In a small sample of stars selected solely on the basis of strong and diverse disk molecular emission, we have found two striking results: (1) the presence of strong UV continuum emission from  $\text{H}_2$  molecules and (2) evidence for grain growth and possible inner disk clearing by planetary bodies. Although our sample is limited we suggest that these two results may be related. The process of grain growth and inner disk clearing will certainly enhance the penetration power of both UV and X-ray radiation, perhaps even leading to regions that are optically thin to UV radiation with penetration only weakly limited by molecular opacity. The direct or improved exposure of molecular gas to high-energy radiation can certainly produce the  $\text{H}_2$  UV emission features seen in our study, which only require a small molecular column ( $<10^{19} \text{ cm}^{-2}$ ; Herczeg et al. 2004). Additional FUV spectra of young T Tauri stars combined with forthcoming *Spitzer Space Telescope* IRS and BASS data on the mid-IR SED will be required to fully determine the relation between FUV emission and grain growth.

Electron impact excitation requires the mixture of hot electrons within an undissociated  $\text{H}_2$  layer (Raymond et al. 1997). For these systems we can assume that the upper layers of the inner disks are mostly cleared of small grains and  $\text{H}_2$  self-shielding limits photodestruction. Under normal circumstances radiation will erode the  $\text{H}_2$  layer, but these systems are still accreting, which provides a source term. In the shielded layer

some hot photoelectrons will be produced via UV ionization of  $\text{C}^+$ , but these do not have sufficient energy ( $\sim 2 \text{ eV}$ ) for  $\text{H}_2$  excitation. Thus, electron excitation likely requires X-ray photons that have greater penetration power and produce higher energy electrons. In the dust-poor inner disk the opacity for abundant 1 keV X-rays will also be reduced by nearly a factor of 3 (Glassgold et al. 1997), allowing X-rays to penetrate into the self-shielded layer, ionize  $\text{H}_2$ , and produce hot electrons mixed within molecular gas. The radiation produced by electron impact excitation of  $\text{H}_2$  therefore does not originate from the star (with an oblique angle of incidence on the disk such as  $\text{Ly}\alpha$ ) but rather arises from the upper layers of the disk itself. This increases the penetration power of the UV radiation with resulting effects on disk physics (UV clearing of inner disk, accretion, gas temperature structure, etc.) and the chemistry of species sensitive to radiation below  $1700 \text{ \AA}$ .

The reduction of dust opacity inside the planet-forming regions of the inner disk along with the presence of gas (inferred from accretion) suggests that some of the heating mechanisms believed important for the outer disk will not be effective in the inner disk. In particular, the efficiency of photoelectric heating can be expected to be reduced and a greater role must be played by X-ray heating and UV-excited  $\text{H}_2$  collisional de-excitation. Thus the gas physics of an evolving inner disk will change as a function of dust evolution. UV emission from  $\text{H}_2$  must trace these changes and provide a direct tracer of the gas conditions within the planet-forming regions of T Tauri disks that are only weakly probed by the dust.

We are grateful for constructive and useful comments from the anonymous referee. E. B. and N. C. are grateful for several discussions with A. Dalgarno. This work has been supported by NASA through grant 09374.01-A from the STScI and Origins of Solar Systems grant NAG5-9670. P. D. acknowledges grants from DGAPA and CONACyT. For this work M. L. S. was supported in part by NASA grant NAG5-9475 and the University Research Council of the University of Cincinnati. D. K. L. and R. W. R. were supported by the Aerospace Corporation's Independent Research and Development program and by the USAF Space and Missile Systems Center through the Mission Oriented Investigation and Experimentation program, under contract F4701-00-C-0009.

#### REFERENCES

- Abgrall, H., Roueff, E., & Drira, I. 2000, *A&AS*, 141, 297  
 Abgrall, H., Roueff, E., Launay, F., & Roncin, J.-Y. 1994, *Canadian J. Phys.*, 72, 856  
 Abgrall, H., Roueff, E., Liu, X., & Shemansky, D. E. 1997, *ApJ*, 481, 557  
 Alibert, Y., Mordasini, C., & Benz, W. 2004, *A&A*, 417, L25  
 Beckwith, S. V. W., Henning, T., & Nakagawa, Y. 2000, in *Protostars and Planets IV*, ed. V. Mannings, A. P. Boss, & S. S. Russell (Tucson: Univ. Arizona Press), 533  
 Bryden, G., Chen, X., Lin, D. N. C., Nelson, R. P., & Papaloizou, J. C. B. 1999, *ApJ*, 514, 344  
 Calvet, N., D'Alessio, P., Hartmann, L., Wilner, D., Walsh, A., & Sitko, M. 2002, *ApJ*, 568, 1008 (C02)  
 D'Alessio, P. 2003, *Rev. Mexicana Astron. Astrofis. Ser. Conf.*, 18, 14  
 D'Alessio, P., Calvet, N., & Hartmann, L. 2001, *ApJ*, 553, 321  
 D'Alessio, P., Calvet, N., Hartmann, L., Lizano, S., & Cantó, J. 1999, *ApJ*, 527, 893  
 Dullemond, C. P., Dominik, C., & Natta, A. 2001, *ApJ*, 560, 957  
 Dutrey, A., Guilloteau, S., & Guelin, M. 1997, *A&A*, 317, L55  
 Glassgold, A. E., Najita, J., & Igea, J. 1997, *ApJ*, 480, 344  
 Herczeg, G. J., Linsky, J. L., Valenti, J. A., Johns-Krull, C. M., & Wood, B. E. 2002, *ApJ*, 572, 310  
 Herczeg, G. J., Wood, B. E., Linsky, J. L., Valenti, J. A., & Johns-Krull, C. M. 2004, *ApJ*, 607, 369  
 Jonin, C., Liu, X., Ajello, J. M., James, G. K., & Abgrall, H. 2000, *ApJS*, 129, 247  
 Kenyon, S. J., & Hartmann, L. 1995, *ApJS*, 101, 117 (KH95)  
 Koerner, D. W., Sargent, A. I., & Beckwith, S. V. W. 1993, *Icarus*, 106, 2  
 Liu, X., Shemansky, D. E., Abgrall, H., Roueff, E., Ahmed, S. M., & Ajello, J. M. 2003, *J. Phys. B*, 36, 173  
 Liu, X., Shemansky, D. E., Abgrall, H., Roueff, E., Dzikczek, D., Hansen, D. L., & Ajello, J. M. 2002, *ApJS*, 138, 229  
 Muzerolle, J., Calvet, N., Hartmann, L., & D'Alessio, P. 2003, *ApJ*, 597, L149 (M03)  
 Qi, C., Kessler, J. E., Koerner, D. W., Sargent, A. I., & Blake, G. A. 2003, *ApJ*, 597, 986  
 Raymond, J. C., Blair, W. P., & Long, K. S. 1997, *ApJ*, 489, 314  
 Rice, W. K. M., Wood, K., Armitage, P. J., Whitney, B. A., & Bjorkman, J. E. 2003, *MNRAS*, 342, 79 (R03)  
 Safronov, V. S. 1972, in *Symp. Origin of the Solar System* (Paris: CNRS), 89  
 Simon, M., Dutrey, A., & Guilloteau, S. 2000, *ApJ*, 545, 1034  
 Sitko, M. L., Lynch, D. K., & Russell, R. W. 2000, *AJ*, 120, 2609  
 Uchida, K. I., et al. 2004, *ApJS*, 154, 439  
 Weidenschilling, S. J. 1997, *Icarus*, 127, 290  
 White, R. J., & Ghez, A. M. 2001, *ApJ*, 556, 265